 DOI: 10.21608/adjalexu.2024.260234.1460

VASCULAR ENDOTHELIAL GROWTH FACTOR WITH AND WITHOUT ALOE VERA IN THE MANAGEMENT OF CLASS II FURCATION DEFECTS IN DOGS

Hadeer M. Mohsen[1*] BDS, Mona Lotfy[2] PhD, Samia Soliman[3] PhD, Gillan I. El-Kimary[4] PhD,

ABSTRACT

AIM: to investigate the effect of Vascular endothelial growth factor(VEGF) with and without Aloe vera in the management of induced critical sized class II furcation defects in dogs using guided tissue regeneration (GTR) approach.

MATERIALS AND METHODS: thirty two critical-sized furcation defects on the buccal surface of mandibular third and fourth premolars were surgically created in eight dogs and divided into two groups. Group I; Sixteen defects were managed using VEGF, aloe vera, β- tricalcium phosphate bone graft (β- TCP) and collagen membrane. Group II; Sixteen defects were managed using VEGF, β- TCP and collagen membrane. Histological and histomorphometric analysis of the newly formed interradicular bone height and its percentage were performed after one and two months.

RESULT: histological examination revealed greater regenerative features in the defects in the second observation period than in the first one. The difference were observed in the forming alveolar bone, cementum thickness, PDL density and fiber orientation. This histological observation were confirmed by the obtained values of the morphometric measurements of the two tested variants

CONCLUSION: VEGF and Aloe vera showed better results than VEGF alone in bone regeneration, cementum thickness, PDL density and fiber orientation. Aloe vera with VEGF have expected to be well established in the field of guided tissue regeneration.

KEYWORDS: Aloe vera, guided tissue regeneration, furcation defect, vascular endothelial growth factor.

RUNNING TITLE: Vascular endothelial growth factor in guided tissue regeneration.

1-B.Sc. in, 2016 Faculty of Dentistry, Pharos University

2-Professor of Oral Medicine, Periodontology, Oral Diagnosis and Oral Radiology Faculty of Dentistry Alexandria University.

3-Professor of Dental Anatomy, Oral Histology and Oral Biology Faculty of Dentistry Alexandria University.

4-Lecturer of Oral Medicine, Periodontology, Oral Diagnosis and Oral Radiology Faculty of Dentistry Alexandria University.

Corresponding author:

Hadeermohamed93@gmail.com

INTRODUCTION

Treating the furcation area in dentistry is challenging due to its extraordinary anatomy, which has important implications for therapy and pathology (1).

Non surgical periodontal therapy (scaling and root planning) with manual and power-driven scalers, open flap debridement (OFD), resective surgery and regenerative approaches have all been proposed as treatment modalities for furcation defects (2,3). The main objective of these therapies is furcation elimination through periodontal regeneration, which promotes the formation of new root cementum, periodontal ligament (PDL), and alveolar bone within the entire furcation area (4).

The bone tissue is highly vascularized. So, rebuilding local microcirculation is required for effective bone regeneration (5). Inhibiting angiogenesis reduces bone formation, whereas promoting angiogenesis improves bone regeneration (6).

Vascular Endothelial Growth Factor (VEGF) is a key regulator of vascular construction and angiogenesis, as well as skeletal development. VEGF also promotes blood artery permeability and is implicated in endothelial cell proliferation, migration, and activation (7).

The vascular growth factor family consists of five members: VEGF-A, VEGF-B, VEGF-C, VEGF-D, and placenta growth factor (PlGF). VEGF-A was the first member of the vascular endothelial growth factor family to be discovered. Vascular endothelial growth factors are important mediators of angiogenesis, which is

required for tumor development and metastasis.(8)

Due to its primary ability to stimulate neovascularization, VEGF is of particular interest in bone regeneration.(8) The VEGF protein can also indirectly differentiate mesenchymal stem cells (MSCs) into the osteogenic lineage. Furthermore, it has a chemokine impact on surrounding endothelial cells (ECs), which might increase the number of vessels in a specific area.(9)

These characteristics help to achieve a more controlled usage of both the stimulating effect of VEGF and the regenerative effects of MSCs. Furthermore, VEGF inhibition has led to non-union models, (9) indicating that the growth factor is critical in the bone healing process.

Gerber et al. (7) studied VEGF's role in angiogenesis and bone formation. Their findings showed that inhibiting VEGF inhibited both vascular invasion and bone formation in 24-day-old mice. It was hypothesized that VEGF could promote ossification by inducing neovascularization or directly affecting bone cells (10).

Herbal medicine is a type of medicine that improves health, prevents disease by using plant roots, stems, leaves, flowers, or seeds. Aloe vera (AV) is a Liliaceae cactus plant with 75 potentially active ingredients, including: vitamins, enzymes, minerals, carbohydrates, lignin, saponins, salicylic acids, amino acids, and polysaccharides (11-13).

Due to its therapeutic qualities such as anti-inflammatory, antibacterial, and antiseptic properties, as well as its potential to induce tissue regeneration, AV is gaining popularity for the treatment of damaged tissues (14,15).

A fundamental reaction to tissue damage is tissue regeneration, which is mainly achieved by the creation of connective tissue matrix. The extracellular matrix (ECM) of connective tissues is primarily composed of collagen. AV was found to increase both the collagen content and the degree of crosslinking in granulation tissue (16).

In a synovial model, AV induces regeneration of fibroblasts and improves tensile strength and collagen turnover in injured tissues (17,18).

Aloe vera has been demonstrated to have antibacterial effect against gram-negative bacteria, which are the major pathogens involved in periodontitis pathogenesis (19). Moreover, AV possesses anti-inflammatory characteristics, which may help to minimize the damage caused by periodontal disease's inflammatory reaction (20).

The aim of this study was to investigate the effect of VEGF with and without AV in the management of induced critical sized class II furcation defects in dogs using GTR approach.

The null hypothesis claimed that there is no significant difference in bone regeneration between the furcation defects treated with VEGF with or without Aloe vera.

MATERIALS AND METHODS

A comparative split mouth experimental study was carried out on a total of eight healthy adult male mongrel dogs (Canis famillaris) aged from 18 to 24 months, weighting approximately between 18 to 24 kg. The sample size was 16 defects per group (number of groups=2) (Total sample size=32 defects). The Faculty of Dentistry at Alexandria University carried it out in accordance with the ethical criteria for conducting research on experimental animals. The animal Ethical Committee of Alexandria University approved this study with the number IRB 00010556-IORG 0008839.

Animals housing was under the same environment and nutrition. An adaptation period of four weeks was allowed before the beginning of the study.

Adopting a power of 80% (β=0.20) to detect a standardized effect size in height of newly formed inter-radicular bone (primary outcome) of 0.47, and level of significance 5% (α error accepted =0.05).The sample size was calculated using G Power version 3.1.9.2 (21).

Materials

β-tricalcium phosphate (β-TCP) alloplast graft (β-tricalcium phosphate (β-TCP), ∗Adbone ®, Medbone Biomaterials, Sintra, Portugal) was used to fill all the furcation defect. Resorbable collagen type 1 membrane, Hypro-Sorb® (Collagen membrane, Hypro-Sorb ®, Giessen, Germany) was used to cover the grafted defect.

Vascular Endothelial Growth Factor 165 (Human VEGF 165 Protein (Recombinant), LSBIO companies, Seattle, United States) was obtained as lyophilized so the vial should centrifuge prior to opening. reconstitute in distilled water at 100 ug/ml is recommended. The size of VEGF 165 used in this study is 50 ug.

AV gel prepared in the laboratories of the Faculty of Pharmacy, Alexandria University. Aloe vera (Aloe barbadensis) leaves were cut lengthwise when they were fresh. Subsequently, the clear gel within was extracted and transformed into a liquid by blending it at 10,000 rpm with a blending machine to remove the fibers. The finished product was kept in a sterile container at 4°C until used (22,23).

Methods

Eight dogs were divided into two groups, each containing sixteen critical-sized furcation defects

that were surgically made on the buccal surface of each mandibular third and fourth premolar (P3, P4) (24). Each of the two groups underwent a split mouth design. Group 1 was managed using VEGF, Aloe vera, (β - TCP) alloplast bone graft and collagen membrane and group 2 was managed using VEGF, β - TCP and collagen membrane.

Surgical procedure

Surgeries were carried out under general anesthesia with intramuscular injections of 0.05 milliliters of xylazine hydrochloride (Xylazine hydrochloride (Alfas an Inc., Holland)) and 0.1 milliliters of ketamine hydrochloride (Ketamine hydrochloride (Bayer Inc. Canada)) per kilogram of body weight . Sulcular incisions were done using a 15 C scalpel and mucoperiosteal flap was reflected by a periostial elevator (Fig. 1A,B). Using carbide surgical burs, thirty-two critical-sized class II furcation defects measuring four millimeters in depth by five millimeters in height were made on the buccal surface of the mandibular third and fourth premolars (P3, P4) in each dog (25) (Fig. 1C). To provide reference points for histologic examination, At the apical end of each defect, two reference notches were cut on the mesial and distal roots. Tetracycline was used for root conditioning after root planning. Sixteen defects of experimental group 1 were managed using 30µl VEGF applied by micropipette (Fig.1 D). After one minute, 30µl Aloe vera was added and two minutes later (Fig. 1 E,F), (β - TCP) alloplast was used to fill the defect and other Sixteen defects of experimental group 2 were managed using 30µl of VEGF which was applied in the defect using a micro-pipette and left for one minute, then (β - TCP) alloplast graft was used to fill the defect (Fig. 1 G). In both groups, collagen membranes were covered the grafted defects extending 2 mm beyond the defect borders (Fig.1 H) (26,27). Then flaps were repositioned and interrupted suturing was used to close the wound area, using 3-0 silk sutures (Ethicon silk suture, Johnson & Johnson, Somerville, NJ) (Fig.1 I).

Postoperative management

Intramuscular antibiotic (Ampicillin) (Eipico, 10th of Ramadan City, Egypt) 3mg/lb of bodyweight was administered twice daily and intramuscular (IM) non-steroidal anti-inflammatory (0.09 mg/lb body weight) (Meloxicam DELTA PHARMA Factory Industrial Zone B4,10th of Ramadan City, Egypt) was administered for all animals for one week (28). Soft diet was served to the during the recovery phase in order to lessen the chance of local trauma to the surgical sites.

Animal euthanize

Four dogs received an intravenous overdose of thiopental sodium injection after one month, and the remaining four dogs received the injection after three months. For histological preparation, the mandible was removed, separated into two halves, and then preserved in 10% neutral buffered formalin (25).

Specimen preparation

The samples were stored in 10% buffered neutral formalin for five days. Subsequently, samples were washed under running water and then put in 8% trichloroacetic acid to decalcify them. Then were progressively dehydrated in increasing concentrations of ethyl alcohol after they had fully decalcified and been rinsed under running water. Then were moved from alcohol using two xylene modifications. Then were embedded in paraffin blocks after being contaminated with paraffin wax. Using the standard procedure, successive mesio-distal slices were sliced and stained with eosin and hematoxylin. Gomori's trichrome dye was used to analyze the new collagen organization and bone development (29-30).

Histomorphometric analysis

Histomorphometric analysis was performed on each sample using the (Image J 1.46r) software (31). The measurements were made by two blinded examiners, and the mean of their results was determined. five mesiodistal slices at various standardized depths were collected from every specimen. One picture was captured using the same magnification level. Every picture was given two parameters:

The height of newly formed inter-radicular bone

The apical ends of the two interradicular dentin notches were connected by a horizontal line. A perpendicular straight line was drawn as well to the previous one, extending all the way to the bifurcation. By selecting set scale from the analyse tab, this line was utilized to set a scale of 5 mm on the photograph to convert pixels to millimeters. A second straight line was established from the apical end of the two notches to the coronal end of the freshly produced bone, and its length was calculated with Image J's measure tab. The same process was followed in each of the five portions of each specimen to determine the mean length. All specimens in each group underwent the same technique.

The percentage of the newly formed bone surface area

Using image J software, a rectangle measuring 2 x 1.5 cm was created on each picture, encompassing the PDL tissues, parts of the two nearby roots, and the interradicular regenerated bone. By choosing the ROI manager from the analysis tools and taking a measurement, the entire surface area of the designated region was determined. The measurements were taken of the two surrounding roots of the tooth, portions of

the PDL, and the surface area occupied by bone marrow using the wand tracing tool.

Total surface area (or overall rectangle measurement) was reduced by the later measurement. Next, the proportion of the entire surface area was computed.

Statistical methodology

Data were obtained and entered into a computer for statistical analysis using the SPSS (Statistical Package for Social Science) program (ver 25) (32). When appropriate, data were entered as either numerical or categorical. Kolmogorov-Smirnov test of normality revealed significance in the distribution of the variables, so the non-parametric statistics was adopted (33). Data were explained using minimum, maximum, median and inter-quartile range for not-normally distributed data. Data were explained using minimum, maximum, median, 95% Confidence Interval of the median, and 25^{th} to 75^{th} percentiles.

Percentage change was calculated as follows:

Percentage change (%)

$$= \frac{\text{Measurement (after)} - \text{Meaurement (before)}}{\text{Meaurement (before)}} \text{ x } 100$$

An 80 percent power of study was allowed for beta error up to 20 percent during the sample size calculation. The alpha level was set at 5%, with a 95% significance level. Statistical significance was calculated using a p value of 0.05 (34).

Histological Results of first observation period

Group 1 (Aloe vera +VEGF+ β -TCP)

The regenerating defects contained considerable amounts of forming bone mostly of the cancellous type. the trabeculae exhibited considerable thickness and enclosed many blood vessels in between them (Fig. 2 A). The latter were of different calibers and were supported by aggregates of β -TCP, Counterrally and deep in the defects, figures of newly formed immature bone were traced with resident union between previously formed ones and intervening figures of β - TCP. (Fig. 2 B)

On the border of the regenerating bone trabeculae, osteoblasts appeared voluminous and were seen the spans between adjacent trabeculae or arranged in double layers. The PDL fibers on both sides of the defects exhibited considerable condensation with sometimes indistinct course from bone to cementum. where they became finally embedded constituting sharpey's fibers .and enclosing between them osteoblasts and cementoblasts respectively. Cementum showed slight variations in it's thickness all over the borders of the defects. (Fig. 2 C-G)

Trichrome stained sections clearly revealed the PDL fiber course and inserion in the bone and cementum as well as the active fibroblasts between the different fiber grouping. (Fig. 2 H)

Group 2 (VEGF + β -TCP)

The regenerating defects contained less amount of forming bone than that of group 1 of the same observation period. This bone was mainly of the cancellous variety and exhibited marked variation in trabeculae thickness and maturation. However the immature figures were prominent. (Fig. 3 A-C)

Defective bone formation was noted in many sections at the defect summit (Fig.3 A), The thickness of the regenerating cementum was great but it contained points of constriction at irregular intervals with structural disorganization appearing as circular or elongated voids lacking any evidence of tissue deposition, Also the incremental lines of salter were irregularly spaced or absent in some of it's segments (Fig. 3 D). In sections of different depth, great degree of tissue vascularity was noted.

Large blood vessels appeared engaged with RBCs and surrounded by mesh works of B-TCP. Many figures of angiogenesis could be traced with sprouting of very small capillaries from large ones (Fig. 3 E, F). The PDL fiber groups appeared condensed and disorganized in their course from bone to cementum. Fibroblasts appeared comprised and flattened among the fiber bundles. small sized osteoblasts and cementoblasts appeared on bone and cementum borders respectively while separated by the inserting fibers which established sharpey's fibers in both tissue. (Fig. 3 G-H)

Histological Results of second observation period

Group 1 (Aloe vera +VEGF+ β -TCP)

The regenerative features of the periodontium in this group was the most effective of all the groups comprised in this research. the interradicular regenerating bone comprised mainly the compact variety with regular borders on both sides with PDL -cementum exhibited regular and constant thickness allover its contact with PDL. the latter showed well organized and dense fiber bundles of typical course from bone to cementum and contained many vascular figures, (Fig. 4 A-D).

At higher level of magnification, the collagen fiber bundles could be followed inserting deeply in both bone and cementum. Establishing sharpey's fibers. Also sizable fibroblasts appeared among the collagen fiber bundles while oriented with the fiber course, (Fig. 4B and Fig. 4 D).

Osteoblastic and cementoblastic activity were a prominent feature especially the osteoblasts which appeared voluminous and arranged in continuous rows on the bone border facing the PDL (Fig. 4 C). Regular rows of active cementoblasts were constantly arranged on

cementum border and rested on a layer of cementoid, (Fig. 4 E)

Trichrome stained sections supported the observation of H&E stained sections and revealed the actual density of PDL fiber and course between bone and cementum as well as their insertion in both tissues, (Fig. 4F).

Group 2 (VEGF + β -TCP)

The signs of periodontium regeneration in this group differed considerably from that of group 1 of the same observation period. The difference were observed in the forming alveolar bone, cementum thickness, PDL density and fiber orientation (Fig. 5 A).

The regenerating bone was predominantly of the cancellous variety with interruption by small masses of β-TCP or their spaces. Most of the formed trabeculae in the coronal portions were of mature type while immature variety could be seen at the apical boundary of the defects where union with the native bone was evident (Fig.5 A).

Un even thickness of cementum was noted at different root segments. PDL fibers facing the bone trabeculae appeared abnormally thickened and exhibited disorganized course and distribution (Fig.5 B).

In association with the appearance of the immature bone at the defect base, continuation of bone formation could bs traced at more coronal segments with extension towards areas of the PDL lacking adjacent normal bone thickness (Fig.5 C).

Activity of osteoblasts and cementoblasts appeared less than in group 1 of the same observation period. Smaller osteoblasts appeared at areas of extension of bone formation. Also small cementoblasts were seen in interrupted rows resting on segments of un even thickness (Fig. 5 D,E).

Insertion of PDL sharpey's fibers in bone appeared more evident than their appearance in association with cementum (Fig. 5 F).

Histomorphometric results

Height of the formed bone in the defects (mm)

One month postoperatively

In the VEGF + Aloe vera + β-TCP Group, the height of the formed bone in the defects (mm) ranged from 3.11 to 3.88 with a median of 3.63, 95% Confidence Interval (CI) of the median of 3.40-3.72 and with Percentile 25th – Percentile 75th of 3.40-3.72 mm. In the VEGF + β-TCP Group (n=16), the height of the formed bone in the defects (mm) ranged from 2.51 to 3.44 with a median of 3.00, 95% CI of the median of 2.83-3.02 and with Percentile 25th – Percentile 75th of 2.82-3.05 mm.

There was a statistically significant difference in the Height of the formed bone in the defects between the two studied groups at one month postoperative (p<.001) (Table 1)

After one month, pairwise comparisons revealed that the Height of the formed bone in the defects was statistically significantly higher in the VEGF + Aloe vera + β-TCP Group, compared to the VEGF + β-TCP Group (p=.005).

Two months postoperatively

In the VEGF + Aloe vera + β-TCP Group (n=16), the height of the formed bone in the defects (mm) ranged from 3.81 to 4.94 with a median of 4.26, 95% CI of the median of 34.20-4.40 and with Percentile 25th – Percentile 75th of 4.19-4.45 mm. In the VEGF + β-TCP Group (n=16), the height of the formed bone in the defects (mm) ranged from 3.30 to 3.82 with a median of 3.43, 95% CI of the median of 3.40-3.76 and with Percentile 25th – Percentile 75th of 3.38-3.76 mm.

There was a statistically significant difference in the Height of the formed bone in the defects among the two studied groups at one month postoperative (p<.001) (Table 1)

After two months, pairwise comparisons revealed that the Height of the formed bone in the defects was statistically significantly higher in the VEGF + Aloe vera + β-TCP Group, compared to the VEGF + β-TCP Group (p=.004).

Percentage of the formed bone in the defects (%)

One month postoperatively

In the VEGF + Aloe vera + β-TCP Group, the Percentage of the formed bone in the defects (%) ranged from 43.88 to 61.44 with a median of 53.86, 95% CI of the median of 49.95-57.49 and with Percentile 25th – Percentile 75th of 49.46-58.56 (%). In the VEGF + β-TCP Group, the Percentage of the formed bone in the defects (%) ranged from 37.05 to 53.86 with a median of 45.68, 95% CI of the median of 40.38-47.92 and with Percentile 25th – Percentile 75th of 39.75-48.13 (%).

There was a statistically significant difference in the Percentage of the formed bone in the defects among the two studied groups at one month postoperative (p<.001) (Table 2).

After one month, pairwise comparisons revealed that the Percentage of the formed bone in the defects was statistically significantly higher in the VEGF + Aloe vera + β-TCP Group, compared to the VEGF + β-TCP Group (p=.015).

Two months postoperatively

In the VEGF + Aloe vera + β-TCP Group, the Percentage of the formed bone in the defects (%) ranged from 69.24 to 90.01 with a median of 77.98, 95% CI of the median of 74.91-78.82 and with Percentile 25th – Percentile 75th of 74.44-80.52 (%). In the VEGF + β-TCP Group,

the Percentage of the formed bone in the defects (%) ranged from 42.80 to 77.43 with a median of 62.03, 95% CI of the median of 55.80-69.07 and with Percentile 25^{th} – Percentile 75^{th} of 55.79-69.59 (%).

There was a statistically significant difference in the Percentage of the formed bone in the defects between the two studied groups at two months postoperative (p<.001) (Table 2).

After two months, pairwise comparisons revealed that the Percentage of the formed bone in the defects was statistically significantly higher in the VEGF + Aloe vera + β-TCP Group, compared to the VEGF + β-TCP Group (p=.006).

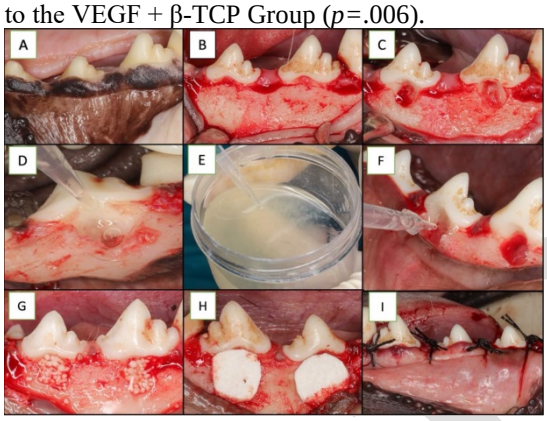

Figure 1: Clinical photographs showing the surgical procedures **(A)**: Mandibular third (P_3) and fourth (P_4) premolars **(B)**: the surgical field after mucoperiosteal elevation **(C):** creation the critical sized class II furcation defects **(D)**: application of VEGF **(E)**: Aloe vera gel **(F)**: application of Aloe vera gel using micropipette. **(G)**: B-TCP was used to fill the defect **(H)**: collagen membrane **(I)**: interrupted sutures

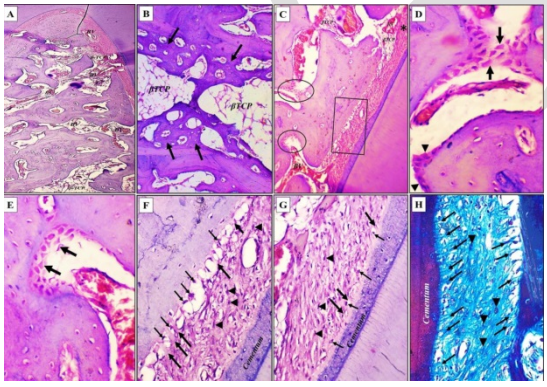

Figure 2: [DSs, one months, Gp. I] A-G: H&E, H: Trichrome **(A):** Showing formation of considerable amount of regenerating bone with great figures of vascularity (BV) and β-TCP, original magnification X: 40. **(B):** segments of newly regenerating bone (arrows) at the edges of previously formed trabeculae. **(C):** Showing noticeable density of the PDL fibers and uneven thickness of cementum allover the border of the defect. X: 100. **(D and E):** Higher magnification of the two encircled areas in the previous figure showing the great activity and proliferation of osteoblasts (arrows) **(D,E)** X: 400.**(F):** Higher magnification illustrating the organization of the PDL fibers and their insertion in the regenerating bone as Sharpeys' fibers (thick arrows). Voluminous osteoblasts are seen at the border of bone between these fibers (thin arrows). X: 400. **(G):** Higher magnification illustrating the organization of the PDL fibers adjacent to the regenerating cementum constituting Sharpeys' fibers (thick arrows). Note the uneven thickness of cementum and embedded cementocytes, X:400. **(H):** showing considerable density of PDL fibers in the central region and uneven thickness of cementum. Insertion of Sharpeys'fibers in both cementum and bone (arrows) is clearly seen, X: 400

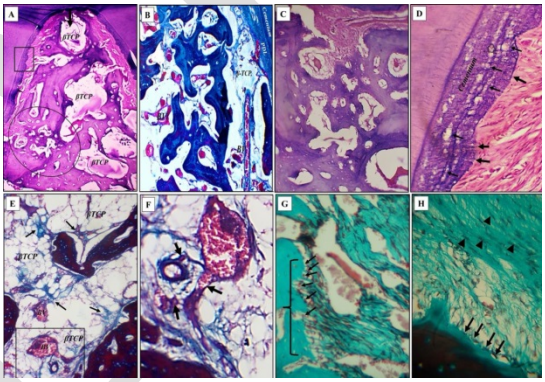

Figure 3: [DSs, one months, Gp.II A,C,D:H&E ,B,E-H: Trichrome:(A):Showing less amount of regenerating bone in comparison to that of Gp.I with greater spaces of β-TCP. Bone trabeculae show variability in thickness and maturation. Cementum exhibits uneven width on both sides of the regenerating defect. X: 40. (B): Showing interconnected trabeculae thinner than those in the previous figure with incomplete maturation. Note the vascularity in the defect (BV) X: 40. (C): Higher magnification showing disorganization of trabecular thickness, connectivity and maturation, X: 100. (D): Showing the abnormal thickness and altered structure of cementum with many voids lacking any deposited tissue (thin arrows), X: 400. (E): many blood vessels (BV) supported by considerable mesh of β-TCP among few figures of forming Bone. Formation of bone collagen fibers is seen extending from already formed bone while supported by β-TCP (arrows), X: 100 (F): Higher magnification of the previous figures revealing sprouting of many small capillaries (arrows) from larger blood vessels establishing angiogenesis, X: 400 (G): showing thickened and disorganized fiber bundles of the PDL. Flattened fibroblasts are seen among the compressed

collagen bundles. Thin sharpey's fibers are seen inserting in bone (brace)with intervening small sized osteoblasts (arrows), X: 400 (H): Showing flattened fibroblasts among the compressed collagen bundles (arrow heads) in the center of the ligament are seen, X:400

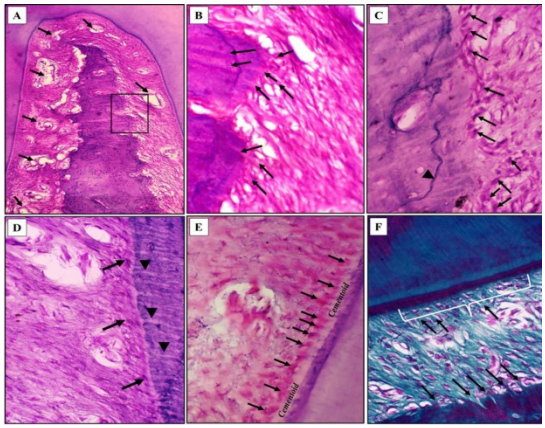

Figure 4: [DSs, two months, Gp.I] A-G :H&E, H :Trichrome stain **(A):** Showing formation of compact bone in the regenerated interradicular defect with regular border adjacent to the PDL, and cementum. Many figures of PDL vascularity are seen (arrows),X: 40.**(B):** Higher magnification of the inset in the previous figure revealing insertion of the regenerating PDL fibers in the bone and their deeper extension into it (arrows), X: 400.**(C):** voluminous osteoblasts arranged in continuous rows adjacent to the border of regenerating bone (arrows), X: 400. **(D):** The insertion of sharpeys' fibers in cementum (arrow), X: 400. **(E):** Continuous row of active cementoblasts (arrows) on the border of cementum while separated from it by a layer of cementoid, X: 400. **(F):** Higher magnification revealing the density of the fiber bundles of the PDL, voluminous fibroblasts and fiber bundle insertion in both cementum and bone (arrows). Note the regular thickness of cementum, and associated cementoblasts (brace), X:400.

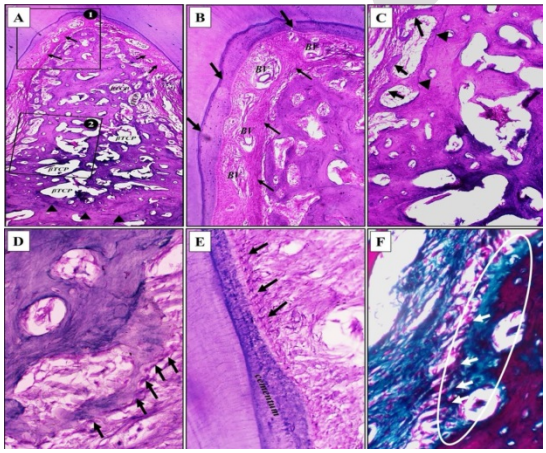

Figure 5: [DS, two months, Gp.II] A-E: H&E, F: Trichrome **(A):** showing considerable density of regenerating bone in the defect with predominance of the cancellous variety(arrow heads), X:40. **(B):**Higher magnification of inset (1) in the previous figure showing uneven thickness of the regenerating cementum (thick arrows) and uneven thickness of the PDL fiber bundles (thin arrows),Profound vascularity of the PDL is seen (BV), X:100.**(C):** Higher magnification of inset (2) in figure A showing the immature bone adjacent to the mature segment, X: 100. **(D):** showing the activity of osteoblasts adjacent to an area of extension of bone formation (arrows), X:400. **(E)**: showing the activity of cementoblasts (arrows), X:400 **(F):** Higher magnification showing an area of new bone formation (circle) in association with new insertion of Sharpeys' fibers (arrows) and accompanied osteoblasts, X:400.

Table 1: Comparison of the height of the formed bone in the defects (mm) at different times of measurements among the two studied groups.

Height of the formed bone in the defects (mm)	VEGF + Aloe vera + β-TCP	VEGF + β-TCP
One month postoperative		
Min. – Max.	3.11-3.88	2.51-3.44
Median	3.63	3.00
95% CI of the median	3.40-3.72	2.83-3.02
Percentile 25th – Percentile 75th	3.33-3.72	2.82-3.05
Two months postoperative		
95% CI of the mean	3.81-4.94	3.30-3.82
Median	4.26	3.43
95% CI of the median	4.20-4.40	3.40-3.76
Percentile 25th – Percentile 75th	4.19-4.45	3.38-3.76
Test of Significance	$Z_{(WSR)}$=3.517	$Z_{(WSR)}$=3.518
p-value	$p<.001$*	$p<.001$*
Percentage Change		
Min. – Max.	11.37-44.71	9.59-35.46
Median	21.59	19.26
95% CI of the median	15.69-25.72	13.40-24.92
Percentile 25th – Percentile 75th	14.30-26.52	13.35-25.37

Table 2: Comparison of the Percentage of the formed bone in the defects (%) at different times of measurements among the two studied groups

Percentage of the formed bone in the defects (%)	VEGF + Aloe vera + β-TCP	VEGF + β-TCP
One month postoperative		
Min. – Max.	43.88-61.44	37.05-53.86
Median	53.86	45.68
95% CI of the median	49.95-57.49	40.38-47.92
Percentile 25th – Percentile 75th	49.46-58.56	39.75-48.13
Two months postoperative		
Min. – Max.	69.24-90.01	42.80-77.43
Median	77.98	62.03
95% CI of the median	74.91-78.82	55.80-69.07
Percentile 25th – Percentile 75th	74.44-80.52	55.79-69.59
Test of Significance	$Z_{(WSR)}$=3.516	$Z_{(WSR)}$=3.516
p-value	*p*<.001*	*p*<.001*
Percentage Change		
Min. – Max.	25.18-78.24	10.00-88.85
Median	50.80	31.99
95% CI of the median	35.44-54.06	15.96-66.44
Percentile 25th – Percentile 75th	33.31-54.37	15.75-68.54

DISSCUSION

The most essential growth factors for regulating vascular development and angiogenesis is vascular endothelial growth factor (VEGF). Given that bone is a highly vascularized tissue and that osteogenesis is largely dependent on angiogenesis, VEGF affects both postnatal bone repair and skeletal development. In the present research we evaluated periodontal regeneration in class II furcation defects using VEGF with and without Aloe vera (AV). The regenerative features were quantitatively and qualitively pronounced in group 1 that was managed using VEGF and Aloe vera including the regenerated bone, cementum, PDL fibers density and organization this result was verified by histological and histomorphometric analysis. In this group, our current results revealed also that there was organized constant rows of cementoblast-like cells, fibroblast and osteoblast. Similar to Al-Hijazi et al. (35) who showed that bone formation and maturation was accelerated by using a combination of AV and VEGF. This proved that AV and VEGF acted as powerful tool for enhancement of bone regeneration. Additionally, the previous study demonstrated that this combination (VEGF and AV) was effective in promoting bone growth, maturation, and enhancement of the overall implant osseointegration.

The bone regenerative capability that found in group 1 might be due to the inductive effect of Aloe vera that induce regeneration of fibroblast and improves tensile strength and collagen turn over in injured tissue. This has been confirmed by the morphometric results in the VEGF + AV + β-TCP Group, one month postoperatively, the height of the formed bone in the defects (mm) ranged from 3.11 to 3.88 with a median of 3.63. Compared to VEGF + β-TCP Group, the height of the formed bone in the defects (mm) ranged from 2.51 to 3.44 with a median of 3.00. However, two months postoperatively, in the VEGF + AV + β-TCP Group, the height of the formed bone in the defects (mm) ranged from 3.81 to 4.94 with a median of 4.26. In the VEGF + β-TCP Group, the height of the formed bone in the defects (mm) ranged from 3.30 to 3.82 with a median of 3.43.

In the current study, the group that managed with VEGF , Aloe Vera and B-TCP showed that the activity of osteoblasts and cementoblasts were prominent feature as osteoblast appeared voluminous and arranged in double layer or formed multiples rows and also active regular rows of cementoblasts were arranged on cementum border . On the other hand , the group that managed with VEGF and B-TCP showed that osteoblast appeared in small sized . Also small cementoblasts were seen in interrupted rows resting on segments of uneven cementum thickness, This is in agreement with P. Chantarawaratit et al. (36) who observed that acemannan can induce extracellular matrix synthesis and the differentiation of PDLCs into hard tissue forming cells, osteoblasts and cementoblasts, which generate bone and cementum, respectively.

The current findings may be explained by the results of the research that examined the effect of topical AV application on bone repair by histological inspection and immunohistochemical evaluation on femur bone defects in Swiss rats (37). Aloe vera has been shown to have the potential to operate as a bioactive molecule that promotes osteoblast development and

proliferation with high bone morphogenetic protein 7 (BMP7) expression, hence causing the production of new bone (37). Furthermore, it has been reported that AV plays a role in tissue repair via one of its constituents, mannose-6-phosphate polysaccharide, which is regarded as an immunostimulant material because it has the ability to stimulate fibroblast replication (38).

The vascularity in the first observation period in group 1 and group 2 was greater than that of the same groups in the second observation period and this may be due to high activity of bone modulation and bone remodleing in the first observation period with subsequent accomdation of vascular area for bone formation.

Based on previously mentioned results, VEGF with AV can be safely utilized in conjunction with bone graft materials. However, further studies are still recommended to evaluate its use in other periodontal defects and to understand the mechanism behind its regenerative potential.

There is a limitation for this study, as further experimental and clinical studies using vascular endothelial growth factor are required and further studies Using VEGF and Aloe vera in different PDL surgeries are recommended. Carrying out researches using VEGF to investigate the cell activity like alkaline phosphatase and others that are expressed in association with cementoblasts and fibroblasts and also cementoblast , fibroblast count osteoblastic count (OC), cementum layer thickness (CLT) and percentage of collagen in bone matrix (CBM).

CONCLUSION

Our data suggest that Aloe Vera could be a candidate biomolecule for tissue regeneration. And a combination of AV with VEGF represent a such a new strategy that might ultimately be applicable to enhance angiogenesis and bone regeneration. This new strategy can be very useful in patients suffer from osteoporosis and blood disorder as well as diabetics patients that complain from delayed healing. Out of the promising results AV with VEGF have shown, it is expected to be well established in the field of guided tissue regeneration.

CONFLICT OF INTEREST

The paper's authors have clarified that they have no conceivable conflicts of interest with the research, authorship, and/or publishing of this paper.

FUNDING

The authors received no monetary compensation for the research, authorship, and/or publication of this paper.

REFERENCES

1. Sanz M, Jepsen K, Eickholz P, Jepsen S. Clinical concepts for regenerative therapy in furcations. Periodontol 2000. 2015;68308-32.
2. Cattabriga M, Pedrazzoli V, Wilson TG Jr. The conservative approach in the treatment of furcation lesions. Periodontol 2000. 2000;22:133-53.
3. Queiroz LA, Santamaria MP, Casati MZ, Ruiz KS, Nociti F Jr, Sallum AW, et al. Enamel matrix protein derivative and/or synthetic bone substitute for the treatment of mandibular class II buccal furcation defects. A 12-month randomized clinical trial. Clin Oral Investig. 2016;20:1597-606.
4. Laugisch O, Cosgarea R, Nikou G, Nikolidakis D, Donos N, Salvi GE, et al. Histologic evidence of periodontal regeneration in furcation defects: a systematic review. Clin Oral Investig. 2019;23:2861-906.
5. Saran U, Gemini Piperni S, Chatterjee S. Role of angiogenesis in bone repair. Arch Biochem Biophys. 2014;561:109-17.
6. Zisch AH, Lutolf MP, Hubbell JA. Biopolymeric delivery matrices for angiogenic growth factors. Cardiovasc Pathol. 2003;12:295-310.
7. Gerber HP, Vu TH, Ryan AM, Kowalski J, Werb Z, Ferrara N. VEGF couples hypertrophic cartilage remodeling, ossification and angiogenesis during endochondral bone formation. Nat Med. 1999;5:623-8.
8. Hoeben ANN, Landuyt B, Highley MS, Wildiers H, Oosterom ATVAN, Bruijn EADE. Vascular endothelial growth factor and angiogenesis 2004;56(4):549–80.
9. Street J, Bao M, DeGuzman L, Bunting S, Peale FV, Ferrara N, et al. Vascular endothelial growth factor stimulates bone repair by promoting angiogenesis and bone turnover. Proc Natl Acad Sci USA 2002 Jul 23;99(15):9656–61 [Internet],
10. Hu K, Olsen BR. The roles of vascular endothelial growth factor in bone repair and regeneration. Bone. 2016;91:30-8.
11. Vickers A, Zollman C, Lee R. Herbal medicine. West J Med. 2001;175:125-8.
12. Atherton P. Aloe vera revisited. Br J Phytother. 1998;4:76-83.
13. Atherton P. The essential Aloe vera: The actions and the evidence. 2nd ed. United States: Mill Enterprises; 1997.
14. Salehi M, Farzamfar S, Bastami F, Tajerian R. Fabrication and characterization of electrospun PLLA/collagen nanofibrous scaffold coated with chitosan to sustain release of aloe vera gel for skin tissue

engineering. Biomed Eng Appl Basis Commun. 2016;28:1650035-42.
15. Silva SS, Popa EG, Gomes ME, Cerqueira M, Marques AP, Caridade SG, et al. An investigation of the potential application of chitosan/aloe-based membranes for regenerative medicine. Acta Biomater. 2013;9:6790-7.
16. Chithra P, Sajithlal GB, Chandrakasan G. Influence of Aloe vera on collagen characteristics in healing dermal wounds in rats. Mol Cell Biochem. 1998;181:71-6.
17. Davis RH, Stewart GJ, Bregman PJ. Aloe vera and the inflamed synovial pouch model. J Am Podiatr Med Assoc. 1992;82:140-8.
18. Davis RH, DiDonato JJ, Johnson RW, Stewart CB. Aloe vera, hydrocortisone, and sterol influence on wound tensile strength and anti-inflammation. J Am Podiatr Med Assoc. 1994;84:614-21.
19. Fani M, Kohanteb J. Inhibitory activity of Aloe vera gel on some clinically isolated cariogenic and periodontopathic bacteria. J Oral Sci. 2012;54:15-21.
20. Surjushe A, Vasani R, Saple DG. Aloe vera: a short review. Indian J Dermatol. 2008;53:163-6.
21. Faul F, Erdfelder E, Lang AG, Buchner A. G* Power 3: A flexible statistical power analysis program for the social, behavioral, and biomedical sciences. Behav Res Methods 2007;39:175-91.
22. Takon IA, Ikpeme EV, Odey MO. Comparative Study of the Antimicrobial Properties of Aloe Vera Juice and Gel (Leaf) Extracts Against Selected Clinical Isolates. Int J Technic Res Appl. 2015;3:108-11.
23. Alkhouli M, Laflouf M, Alhaddad M. Efficacy of Aloe-Vera Use for Prevention of Chemotherapy-Induced Oral Mucositis in Children with Acute Lymphoblastic Leukemia: A Randomized Controlled Clinical Trial. Compr Child Adolesc Nurs. 2021;44:49-62.
24. Ibrahim M, Khalil NM, Fahmy RA. Management of Class II furcation defects in dogs using combination of Propolis and Nanobone graft. Egypt Dent J. 2019;65:3365-74.
25. Afifi MM, Kotry GS, El-Kimary GI, Youssef HA. Immunohistopathologic evaluation of Drynaria fortunei rhizome extract in the management of Class II furcation defects in a canine model. J Periodontol. 2018;89:1362-71. 262
26. Firdaus I, Arfian N, Wahyuningsih MS, Agustiningsih D. Aloe vera stimulate cell proliferation, cell migration, expression of vascular endothelial growth factor-A (VEGF-A), and c-Jun N-terminal kinase-1 (JNK-1) on fibroblast of diabetic rat models. Berkala Ilmu Kedokteran. 2019;51:114-27.
27. Du B, Liu W, Deng Y, Li S, Liu X, Gao Y, et al. Angiogenesis and bone regeneration of porous nano-hydroxyapatite/coralline blocks coated with rhVEGF165 in critical-size alveolar bone defects in vivo. Int J Nanomedicine. 2015;10:2555-65.
28. Faul F, Erdfelder E, Lang AG, Buchner A. G* Power 3: A flexible statistical power analysis program for the social, behavioral, and biomedical sciences. Behav Res Methods. 2007;39:175-91.
29. Carleton HM. Carleton's Histological technique. Drury RAB, Wallington EA, editors. Oxford ; New York: Oxford University Press; 1980.
30. GoMori G. A Rapid One-Step Trichrome Stain*. American Journal of Clinical Pathology. 1950;20(7_ts):661-4.
31. Nanes BA. Slide Set: Reproducible image analysis and batch processing with ImageJ. Biotechniques. 2015;59:269-78.
32. IBM Corp. IBM SPSS Statistics for Windows, Version 25.0. Armonk, NY: IBM Corp.; Released 2017.
33. Field A. Discovering Statistics Using IBM SPSS Statistics. 4th ed. London, California, New Delhi: SAGE Publications Ltd; 2013.
34. Curran-Everett D. Evolution in statistics: P values, statistical significance, kayaks, and walking trees. American Physiological Society Bethesda, MD; 2020. p. 221-4.
35. Al-Hijazi AY, Akram ZM, Abdulla EH. Combination Use of Aloe Vera and VEGF Promotes Osseointegration and Stability of Titanium Implants. Indian J Forensic Med Toxicol. 2020;14:2019.
36. Chantarawaratit, P., Sangvanich, P., Banlunara, W., Soontornvipart, K., & Thunyakitpisal, P. (2013). *Acemannan sponges stimulate alveolar bone, cementum and periodontal ligament regeneration in a canine class II furcation defect model. Journal of Periodontal Research, 49(2), 164–178.* doi:10.1111/jre.12090
37. Al-Hijazi AY, Al-Mahammadawy AKA, Altememe EI. Expression of bmp7 in bone tissue treated with aloe vera. Int Res J Nat Sci. 2015;3:39-48.
38. Aro AA, Nishan U, Perez MO, Rodrigues RA, Foglio MA, Carvalho JE, et al. Structural and biochemical alterations during the healing process of tendons treated with Aloe vera. Life Sci. 2012;91:885-93.